Particle dynamics in storage rings with barrier rf systems

S. Y. Lee* and K. Y. Ng
Department of Accelerator Physics, Fermilab, Box 500, Batavia, Illinois 60510
(Received 22 October 1996)

The stability of particle motion in a barrier rf system is studied. Parametric resonance strength functions for the barrier rf system with rf phase and voltage modulations are derived. We find that higher order parametric resonances of the barrier rf system are important. Tolerance of the rf phase modulational errors in the barrier rf system in the Fermilab Recycler, a cooling storage ring to recycle unused antiprotons from the Tevatron and to store newly produced cooled antiprotons, is analyzed. A constraint on the rate of bunch compression utilizing the barrier rf system is derived. [S1063-651X(97)15905-0]

PACS number(s): 29.20.Dh, 03.20.+i, 05.45.+b

I. INTRODUCTION

Bunch beam manipulations have become a routine operational practice in antiproton production, beam coalescence, multiturn injection, accumulation, etc. The demand of higher beam brightness in storage rings and higher luminosity in high energy colliders requires intricate beam manipulations. In particular, a flattened rf wave form has been commonly employed to shape the bunch distribution in order to alleviate space charge problems in low energy proton synchrotrons, and to increase the tune spread in electron storage rings.

For achieving high luminosity in the Fermilab TeV collider Tevatron, a machine called the Recycler has been proposed to recycle unused antiprotons from the Tevatron [1]. The recycled antiprotons can be cooled by stochastic cooling or electron cooling to attain a high phase space density. At the same time, the Recycler also accumulates newly produced, cooled antiprotons from the antiproton Accumulator. To maintain the antiproton bunch structure, a barrier rf wave form [2] is generated to confine the beam bunch, and shape the bunch distribution waiting for the next collider refill. The required bunch length and the momentum spread of the beam can be adjusted more easily by gymnastics with barrier rf waves than the usual rf cavities.

The barrier rf wave is normally generated by a solid state power amplifier, which has intrinsic wide bandwidth characteristics. An arbitrary voltage wave form can be generated across a wideband cavity gap. Figure 1 shows some possible barrier rf waves with half sines and triangular and square function forms. These wave forms are characterized by a voltage amplitude $V(\tau)$, a pulse duration T_1, a pulse gap T_2 between the positive and negative voltage pulses, and an integrated pulse strength $\int V(\tau)d\tau$. For example, the integrated pulse strength for a square wave form is $V_0 T_1$. The rf wave form is applied to a wideband cavity with a frequency $hf_{\rm rev}$, where h is an integer, $f_{\rm rev}$ is the revolution frequency of synchronous particles, whose revolution frequency synchronize with the rf frequency. The effect on the beam is determined mainly by the integrated voltage of the rf pulse. Acceleration or deceleration of the beam can be achieved by employing a biased voltage wave on top of the bunch-confining positive and negative voltage pulses.

Most of the time, orbiting particles see no cavity field in passing through the cavity gap. When a particle travels in the time range where the rf voltage is not zero, the energy of the particle can increase or decrease depending on the sign of the voltage it sees. In this way, the accelerator is divided into stable and unstable regions. Thus the wide bandwidth rf wave can create barrier bucket to confine orbiting particles.

Because solid state amplifiers are normally low power devices, the voltage across the rf gap is usually limited. The resulting bunch area may nearly fill the *bucket area*, which is the maximum stable area that can normally confine the beam particles. Since the bucket is almost full, timing jitter in the rf wave may cause problems in beam stability. In particular, when the frequency spectrum of these perturbations is near a harmonic of the synchrotron frequency, beam particles can be coherently excited to escape the bucket [3–8].

This paper studies the beam dynamics associated with a barrier bucket. We analyze the stability of the particle motion in a barrier bucket under the perturbative force of rf phase and voltage modulations. Furthermore, if the dipole

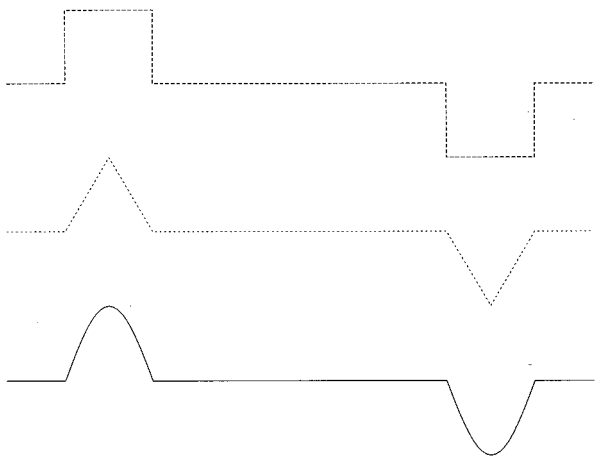

FIG. 1. Possible wave forms for the barrier bucket. The barrier rf wave is characterized by a voltage height V_0, a pulse width T_1, and a pulse gap T_2. Below the transition energy with $\eta<0$, particles are confined within the positive and negative pulse regions. Above the transition energy, the sign of the voltage wave should be reversed.

*Permanent address: Department of Physics, Indiana University, Bloomington, IN 47405.

field in the accelerator is modulated, the resulting circumference of the orbiting particles will be changed as well. This results in a synchrotron phase dependence on the modulating dipole field error, i.e., a kind of synchrobetatron coupling [4,5]. Section II gives fundamental properties of particle motion in the barrier bucket. Section III analyzes the stability of the barrier bucket in the presence of rf phase modulation. Section IV analyzes the effects of rf voltage modulation. Section V discusses the tolerance of the barrier rf cavity in the Recycler, the tolerance of the orbit stability due to synchrobetatron coupling, and the rate of bunch compression with the preservation of the bunch area. The conclusion is given in Sec. VI.

II. PROPERTIES OF THE BARRIER BUCKET

The fractional change of the orbiting time $\Delta T/T_0$ for a particle with an energy deviation ΔE is given by

$$\frac{\Delta T}{T_0}=\eta\frac{\Delta E}{\beta^2E_0}, \tag{2.1}$$

where η is the phase slip factor, and βc and E_0 are, respectively, the speed and energy of the synchronous particle, and T_0 its revolution period. Without loss of generality, we consider synchrotron motion with $\eta<0$ in this paper. For $\eta>0$, the wave form of the barrier bucket is reversed. Let $-\tau$ be the relative time between an off-momentum particle and the synchronous particle at the center of the bucket. The equation of motion for the phase space coordinate τ is

$$\frac{d\tau}{dt}=-\eta\frac{\Delta E}{\beta^2E_0}, \tag{2.2}$$

Passing through a barrier wave, the particle gains energy at the rate of

$$\frac{d(\Delta E)}{dt}=\frac{eV(\tau)}{T_0}. \tag{2.3}$$

Equations (2.2) and (2.3) constitute the equations of motion of a particle in a barrier rf wave.

Since the effect of the barrier rf wave on particle motion depends essentially on the integrated rf voltage wave (see Appendix A), we consider only the square wave forms with voltage heights $\pm V_0$ and a pulse width T_1 in time, separated by a gap of T_2. At a proper passage time, the particle gains or loses equal amount of energy eV_0, i.e., $d(\Delta E)/dt=eV_0/T_0$ every turn. The number of cavity passages before the particle loses all its maximum off-energy value $\widehat{\Delta E}$ is

$$N=\frac{|\widehat{\Delta E}|}{eV_0}. \tag{2.4}$$

Thus the phase space trajectory for a particle with a maximum off-energy $\widehat{\Delta E}$ is given by

$$(\Delta E)^2=\begin{cases}(\widehat{\Delta E})^2 & \text{if } |\tau|\leqslant\dfrac{T_2}{2}\\[2ex] (\widehat{\Delta E})^2-\left(|\tau|-\dfrac{T_2}{2}\right)\dfrac{\omega_0\beta^2E_0eV_0}{\pi|\eta|} & \text{if } \dfrac{T_2}{2}\leqslant|\tau|\leqslant\dfrac{T_2}{2}+T_1,\end{cases} \tag{2.5}$$

where $\omega_0=2\pi f_{\rm rev}$ is the angular revolution frequency of the beam. The phase space ellipse is composed of a straight line in the rf gap region and a parabola in the square rf wave region. The phase space area of the invariant phase space ellipse is

$$\mathcal{A}=2T_2\widehat{\Delta E}+\frac{8\pi|\eta|}{3\omega_0\beta^2E_0eV_0}(\widehat{\Delta E})^3. \tag{2.6}$$

The maximum energy deviation or the barrier height that the barrier rf wave can sustain is given by

$$\Delta E_b=\left(\frac{eV_0T_1}{T_0}\frac{2\beta^2E_0}{|\eta|}\right)^{1/2}, \tag{2.7}$$

where T_1 is the pulse width of the rf voltage wave, and T_0 is the revolution period of the beam. The bucket height depends on V_0T_1, which is the integrated rf voltage strength $\int V(\tau)d\tau$. The synchrotron period is given by

$$T_s=2\frac{T_2}{|\eta|}\left(\frac{\beta^2E_0}{|\widehat{\Delta E}|}\right)+4\frac{|\widehat{\Delta E}|}{eV_0}T_0 \tag{2.8}$$

for a particle inside the bucket. The mathematical minimum synchrotron period of Eq. (2.8) is given by

$$T_{s,\min}=\left(\frac{32T_0T_2\beta^2E_0}{|\eta|eV_0}\right)^{1/2}, \tag{2.9}$$

and the corresponding maximum synchrotron tune is given by

$$\nu_{s,\max}=\left(\frac{T_0}{T_2}\frac{|\eta|eV_0}{32\beta^2E_0}\right)^{1/2}. \tag{2.10}$$

Note here that $\pi T_0/(16T_2)$ plays the role of harmonic number ''h'' of a regular rf system. The synchrotron tune is a function of the off-energy parameter $\widehat{\Delta E}$ given by

$$\nu_s=4\nu_{s,\max}\left(\frac{T_1}{T_2}\right)^{1/2}\frac{\widehat{\Delta E}}{\Delta E_b}\left(1+4\left[\frac{\widehat{\Delta E}}{\Delta E_b}\right]^2\frac{T_1}{T_2}\right)^{-1}. \tag{2.11}$$

Note that when the rf pulse gap width decreases to $T_2/T_1<4$, the synchrotron tune becomes peaked at an amplitude within the bucket height. This feature is similar to

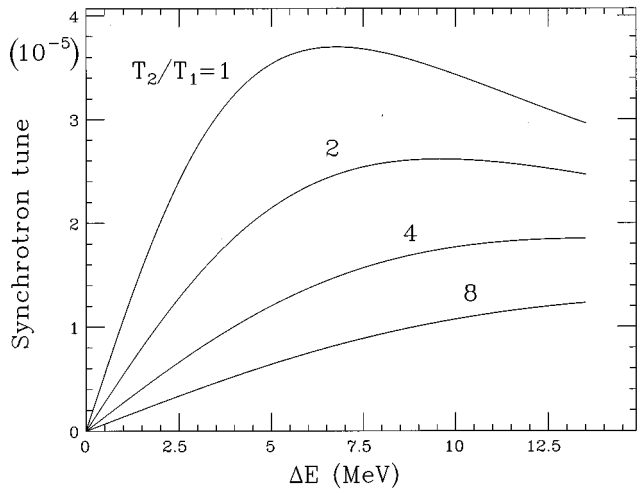

FIG. 2. The synchrotron tune vs the off-energy parameter ΔE. The parameters used in this plot are $E_0=8.9$ GeV, $f_{\rm rev}=89.8$ kHz, $V_0=2$ kV, $\gamma_T=20.7$, and $T_1=0.5$ μs. Note that if $T_2>4T_1$, the synchrotron tune is a monotonic function of ΔE. On the other hand, if $T_2<4T_1$, the synchrotron tune is peaked at an off-energy ΔE smaller than the bucket height ΔE_b.

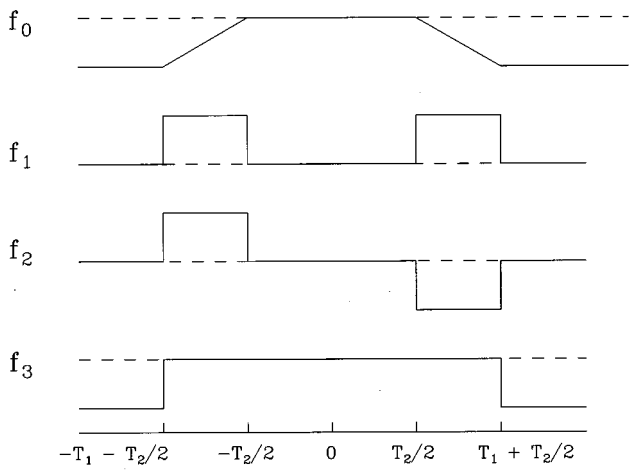

FIG. 3. Schematic drawing of the form factors f_0, f_1, f_2, and f_3 used in this paper for the barrier rf system.

that of a double rf system [7]. Figure 2 shows ν_s vs ΔE with the Fermilab Recycler's parameters $E_0=8.9$ GeV, $\gamma_T=20.7$, $f_{\rm rev}=89.8$ kHz, $T_1=0.5$ μs, $V_0=2$ kV, and $T_2/T_1=1$, 2, 4, and 8 respectively. For example, $\nu_{s,\max}=3.7\times10^{-5}$ for $T_2=T_1$, i.e., the synchrotron frequency is 3.3 Hz.

The Hamiltonian for the phase space coordinates $(\tau,\Delta E)$ is given by

$$H_0=\frac{\eta}{2\beta^2E_0}(\Delta E)^2+\frac{\omega_0eV_0T_1}{2\pi}f_0(\tau,T_1,T_2), \quad (2.12)$$

where

$$f_0(\tau,T_1,T_2)=\frac{1}{T_1}\left[\left(\tau+T_1+\frac{T_2}{2}\right)\theta\left(\tau+T_1+\frac{T_2}{2}\right)-\left(\tau+\frac{T_2}{2}\right)\theta\left(\tau+\frac{T_2}{2}\right)-\left(\tau-\frac{T_2}{2}\right)\theta\left(\tau-\frac{T_2}{2}\right)+\left(\tau-T_1-\frac{T_2}{2}\right)\theta\left(\tau-T_1-\frac{T_2}{2}\right)\right]-1. \quad (2.13)$$

Here $\theta(x)$ is the standard step function with $\theta(x)=1$ for $x>0$ and $\theta(x)=0$ for $x<0$. The top plot of Fig. 3 shows a schematic drawing of the f_0 function.

For constants T_1, T_2, and V_0, the Hamiltonian H_0 is a constant of motion. The action of a Hamiltonian torus is given by

$$J=\frac{1}{2\pi}\oint \Delta E\, d\tau =\frac{1}{2\pi}\left(\frac{\omega_0\beta^2E_0eV_0}{\pi|\eta|}\right)^{1/2}\oint\sqrt{W+f_0(\tau,T_1,T_2)}\,d\tau. \quad (2.14)$$

The parameter W with a dimension of time is related to the Hamiltonian value by

$$H_0=-\frac{\omega_0eV_0}{2\pi}W=\frac{\eta}{2\beta^2E_0}(\widehat{\Delta E})^2. \quad (2.15)$$

For a given Hamiltonian torus, W has the physical meaning that it is equal to the maximum phase excursion $|\tau|$ in the rf wave region. Therefore $W=0$ corresponds to an on-momentum particle, and $W=T_1$ is associated with particles on the bucket boundary.

The action for a particle torus inside the bucket is given by

$$J=\frac{1}{2\pi}\left(\frac{\omega_0\beta^2E_0eV_0}{\pi|\eta|}\right)^{1/2}\left[2T_2\sqrt{W}+\frac{8}{3}W^{3/2}\right] =\frac{1}{2\pi}\left[2T_2+\frac{8}{3}W\right]\widehat{\Delta E}. \quad (2.16)$$

The bucket area is related to the maximum action with $W=T_1$, i.e.,

$$\mathcal{B}=2\pi\hat{J}=(2T_2+\tfrac{8}{3}T_1)\Delta E_b. \quad (2.17)$$

Again, the bucket area depends only on the integrated rf voltage strength $\int V(\tau)d\tau=V_0T_1$.

Canonical transformation from the phase space coordinates $(\tau,\Delta E)$ to the action-angle variable can be achieved by using the generating function

$$F_2(J,\tau)=\int_{-\hat{\tau}}^{\tau}\Delta E\,d\tau, \quad (2.18)$$

where $\hat{\tau}=W+(T_2/2)$. The angle variable ψ is given by

$$\psi=\frac{\partial F_2}{\partial J}=\frac{\pi\sqrt{W}}{T_2+4W}\int_{-\hat{\tau}}^{\tau}\frac{d\tau}{\sqrt{W+f_0}}. \quad (2.19)$$

The integral can be evaluated easily to obtain

$$\psi=\begin{cases}\dfrac{2\pi\sqrt{W}}{T_2+4W}\left(W+\dfrac{T_2}{2}+\tau\right)^{1/2} & \text{if } -W-\dfrac{T_2}{2}\leqslant\tau\leqslant-\dfrac{T_2}{2},\quad \Delta E>0\\ \psi_c+\dfrac{\pi}{T_2+4W}\left(\tau+\dfrac{T_2}{2}\right) & \text{if } -\dfrac{T_2}{2}\leqslant\tau\leqslant\dfrac{T_2}{2},\quad \Delta E>0\\ 2\psi_c+\psi_s-\dfrac{2\pi\sqrt{W}}{T_2+4W}\left(W+\dfrac{T_2}{2}-\tau\right)^{1/2} & \text{if } \dfrac{T_2}{2}\leqslant\tau\leqslant W+\dfrac{T_2}{2},\quad \Delta E>0\\ 2\psi_c+\psi_s+\dfrac{2\pi\sqrt{W}}{T_2+4W}\left(W+\dfrac{T_2}{2}-\tau\right)^{1/2} & \text{if } \dfrac{T_2}{2}\leqslant\tau\leqslant W+\dfrac{T_2}{2},\quad \Delta E<0\\ 3\psi_c+\psi_s+\dfrac{\pi}{T_2+4W}\left(\dfrac{T_2}{2}-\tau\right) & \text{if } -\dfrac{T_2}{2}\leqslant\tau\leqslant\dfrac{T_2}{2},\quad \Delta E<0\\ 4\psi_c+2\psi_s-\dfrac{2\pi\sqrt{W}}{T_2+4W}\left(W+\dfrac{T_2}{2}+\tau\right)^{1/2} & \text{if } -W-\dfrac{T_2}{2}\leqslant\tau\leqslant-\dfrac{T_2}{2},\quad \Delta E<0,\end{cases}\tag{2.20}$$

where

$$\psi_c=\frac{2\pi W}{T_2+4W},\quad \psi_s=\frac{\pi T_2}{T_2+4W}\tag{2.21}$$

are the synchrotron phase advance for a half orbit in the rf wave region and the synchrotron phase advance in the region between two rf pulses respectively. Note that $2\psi_c+\psi_s=\pi$ for one half of the synchrotron orbit; and the motion of a stable particle orbit in the barrier bucket with $\eta<0$ is clockwise. We choose the convention of $\dot{\psi}>0$ corresponding to a clockwise motion in synchrotron phase space.

III. rf PHASE MODULATIONS

Noise in the rf system and ground vibration are inherent in all realistic storage rings. The timing jitter of the rf pulse introduces rf phase modulation, and the variation of the rf voltage, gives rise to amplitude modulation. Furthermore, ground vibration can result in orbit length modulation, which leads to rf phase modulation. This section studies the effects of rf phase errors on stability of the barrier rf system. Possible forms of rf phase error are listed as follows: (1) Breathing rf phase modulation with $T_2\rightarrow T_2+a_1\cos\omega_m t$, (2) rf phase modulation with $\tau\rightarrow\tau+a_2\cos\omega_m t$, (3) rf pulse width modulation with $T_1\rightarrow T_1+a_3\cos\omega_m t$.

A. Breathing rf phase modulation

For case (1), the Hamiltonian can be expressed as

$$H=H_0+\frac{a_1}{2T_1}\frac{eV_0T_1}{T_0}f_1(\tau,T_1,T_2)\cos\omega_m t+\cdots,\tag{3.1}$$

where higher order perturbation terms involving δ function are neglected, and

$$f_1(\tau,T_1,T_2)=\theta\left(\tau+T_1+\frac{T_2}{2}\right)-\theta\left(\tau+\frac{T_2}{2}\right)+\theta\left(\tau-\frac{T_2}{2}\right)-\theta\left(\tau-T_1-\frac{T_2}{2}\right)\tag{3.2}$$

is also schematically shown in Fig. 3. Note that the effective perturbation is proportional to a_1/T_1. We expand the function f_1 in action-angle variables, i.e.,

$$f_1(\tau,T_1,T_2)=\sum_{-\infty}^{\infty}g_m(J)e^{im\psi},\tag{3.3}$$

where

$$g_m=\frac{1}{2\pi}\int_0^{2\pi}f_1(\tau,T_1,T_2)e^{-im\psi}d\psi.\tag{3.4}$$

Since f_1 is a real even function of τ, all odd harmonics vanish with $g_{-m}=g_m^*$. The strength function g_m is given by

$$g_m=\begin{cases}0 & \text{if } m=\text{odd}\\ \dfrac{2}{m\pi}\sin m\psi_c & \text{if } m=\text{even},\end{cases}\tag{3.5}$$

where ψ_c is the phase advance of synchrotron motion across the rf wave region given by Eq. (2.21). Note that the resonance strength function decreases slowly with the mode number m. For a larger T_2 parameter, the resonance strength function also becomes smaller. The resonance strength function satisfies the sum rule theorem

$$\sum_{n=1}^{\infty}|g_{2n}(J)|^2=\frac{2WT_2}{(T_2+4W)^2}.\tag{3.6}$$

The sum rule vanishes for on-momentum particles with $W=0$. Since $W\leqslant T_1$, the sum rule is maximum at orbits with $W=T_2/4$ provided that $T_2\leqslant 4T_1$. For barrier rf systems with $T_2>4T_1$, the sum rule is a monotonic increasing function of the synchrotron amplitude.

The perturbation term in the Hamiltonian becomes

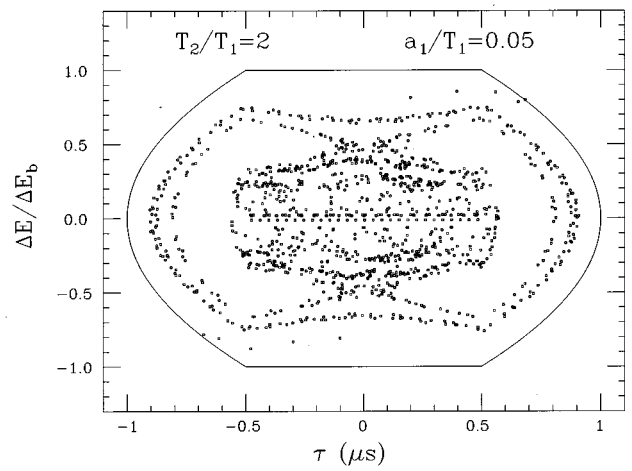

FIG. 4. The Poincaré surface of section at $\omega_m = 1.95\omega_{s,\max}$. The 2:1 parametric resonance generated by the rf breathing phase modulation with $a_1/T_1 = 0.05$ and $T_2/T_1 = 2$. Note that the last torus is about 60% of the bucket height shown as solid lines. Orbits outside the last torus are not bounded by the barrier bucket.

$$\Delta H = \frac{2a_1 WeV_0}{T_0(T_2+4W)}\cos\omega_m t + \sum_{n=1}^{\infty}\frac{a_1 eV_0}{2n\pi T_0}\sin(2n\psi_c) \times[\cos(2n\psi+\omega_m t)+\cos(2n\psi-\omega_m t)]. \quad (3.7)$$

Note here that when the modulation frequency is equal to an even harmonic of the synchrotron frequency, the rf phase modulation can coherently perturb particle motion. Figure 4 shows the Poincaré surface of section [9] for a particle with $a_1/T_1 = 0.05$, $T_2/T_1 = 2$, and a modulation frequency $\omega_m/\omega_{s,\max} = 1.95$, where $\omega_{s,\max} = \omega_0\nu_{s,\max}$ is the maximum angular synchrotron frequency of the rf system. Note that the 2:1 parametric resonance plays an important role in determining the orbit stability, where orbits outside the last torus shown in Fig. 4 are unstable.

To estimate the tolerance of the rf phase breathing modulation, we calculate the maximum stable bunch area of the rf system. We randomly and uniformly populate 1000 particles inside the bucket area and track the beam bunch for more than 50 synchrotron periods. The stable phase space area (in units of the bucket area) is defined as the ratio between the number of survival particles and the number of initial particles. Figure 5 shows the maximum stable bunch area (in ratio to the bucket area) vs the rf phase modulation frequency (in ratio to the maximum synchrotron frequency) with $a_1 = 0.10T_1$, $T_2/T_1 = 4$, where we have $g_4 = 0$, $g_8 = 0$, etc. for the particle orbit on the bucket boundary with $W = T_1$. This fact is reflected in a weak 4:1 parametric resonance shown in Fig. 5. Because the driving amplitude is large in this example, the 8:1 and 12:1 resonances are found not to be small.

In general, a 5% timing jitter gives a stable bunch area of about 95% of the bucket area, provided that parametric resonances are avoided. On the other hand, if the modulation frequency is near a synchrotron sideband, the stable phase space area becomes very small. Figure 6 shows the stable phase space area (in ratio to the bucket area) vs the modulation frequency (in ratio to the maximum synchrotron frequency) with $T_2 = T_1$ and $a_1/T_1 = 0.04, 0.08, \ldots, 0.20$ in steps of 0.04. In order to eliminate high order modes and retain about 90% of stable phase space area near the 2:1 parametric resonance, the modulation amplitude must be $a_1/T_1 \leqslant 0.005$.

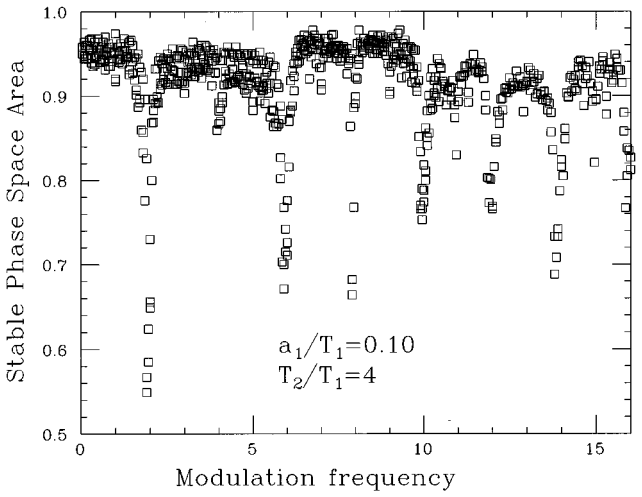

FIG. 5. The stable rf bunch area (in ratio to the bucket area) is plotted as a function of the rf breathing phase modulation frequency (in ratio to the maximum rf frequency). The modulation amplitude is 5% of the rf pulse width, i.e., $a_1/T_1 = 0.05$. The ratio between the rf pulse gap and the pulse width is $T_2/T_1 = 4$. In this example, a smaller resonance excitation at 4:1, 8:1, ... parametric resonances is due to the vanishing $g_4, g_8, \ldots$ on the barrier orbits.

B. Phase modulation of the rf wave

If the entire rf wave timing and/or the particle orbit length are modulated, the effect gives rise to a modulation of the phase variable τ. In this case, the Hamiltonian can be expressed as

$$H = H_0 + \frac{a_2}{T_1}\frac{eV_0T_1}{T_0}f_2(\tau,T_1,T_2)\cos\omega_m t + \cdots, \quad (3.8)$$

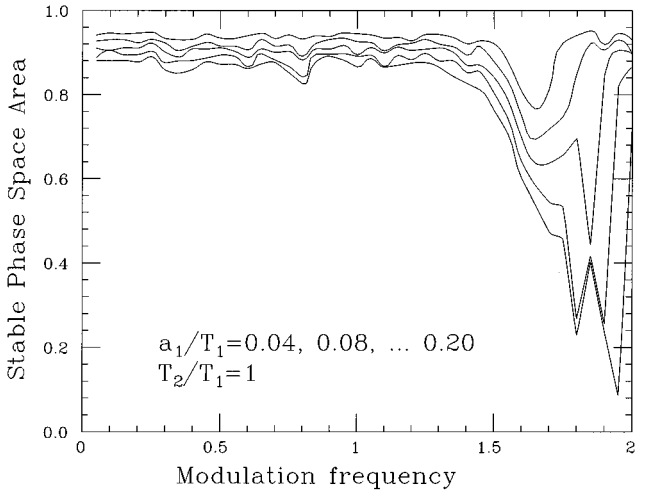

FIG. 6. The stable phase space area (in units of the bucket area) vs the modulation frequency (in units of the maximum synchrotron frequency) for the breathing rf phase modulation with $T_2 = T_1$ and $a_1/T_1 = 0.04, 0.08, \ldots, 0.20$.

where higher order perturbation terms involving δ function are neglected, and

$$f_2(\tau,T_1,T_2)=\theta\left(\tau+T_1+\frac{T_2}{2}\right)-\theta\left(\tau+\frac{T_2}{2}\right)-\theta\left(\tau-\frac{T_2}{2}\right)+\theta\left(\tau-T_1-\frac{T_2}{2}\right) \tag{3.9}$$

is an odd function of τ shown in Fig. 3. The effective phase modulation strength is proportional to a_2/T_1. We expand the function f_2 in action-angle variables, i.e.,

$$f_2(\tau,T_1,T_2)=\sum_{-\infty}^{\infty} h_m(J)e^{im\psi}. \tag{3.10}$$

Since f_2 is an odd function of τ, we obtain

$$h_m=\begin{cases} 0 & \text{if } m=\text{even} \\ \dfrac{2}{m\pi}\sin m\psi_c & \text{if } m=\text{odd.}\end{cases} \tag{3.11}$$

The resonance strength function satisfies the sum rule theorem

$$\sum_{n=1}^{\infty}|h_{2n+1}(J)|^2=\frac{2W}{T_2+4W}. \tag{3.12}$$

The sum rule strength for the rf phase modulation is slightly larger than that of rf breathing phase modulation of Eq. (3.6). This means that the rf phase modulation can cause more particle orbit distortion than the rf breathing phase modulation. The sum rule is a monotonic function of the synchrotron amplitude. At the maximum synchrotron amplitude with $W=T_1$, the sum rule decreases with increasing T_2/T_1.

The perturbation term in the Hamiltonian becomes

$$\Delta H=\sum_{n=1}^{\infty}\frac{a_2eV_0}{(2n+1)\pi T_0}\sin((2n+1)\psi_c)\times[\cos((2n+1)\psi+\omega_m t)+\cos((2n+1)\psi-\omega_m t)] \tag{3.13}$$

When the modulation frequency is equal to an odd harmonic of the synchrotron frequency, particle motion will be strongly perturbed. The resulting effects on particle motion are similar to that discussed in Sec. III A. Figure 7 shows the stable phase space area (in units of the bucket area) vs the modulation frequency (in units of the maximum synchrotron frequency) for $a_2/T_1=0.10$. The reduction of stable bunch area by the excitation of odd order modes is clearly visible.

Figure 8 shows the stable phase space area near the 1:1 parametric resonance for $a_2/T_1=0.01,0.02,\ldots,0.10$, respectively. In comparison with the result of Fig. 6, the loss of phase space area due to the shaking phase modulation is more severe than that of breathing phase modulation.

The top plot of Fig. 9 shows the stable phase area (in units of the bucket area) as a function of the breathing phase modulation amplitude (a_1/T_1) at the 2:1 parametric resonance. The bottom plot shows the stable phase space area vs the shaking phase modulation amplitude a_2/T_1 at the 1:1 parametric resonance. The circles (connected by a solid line) and rectangles are obtained from the parameters $T_2/T_1=1$ and 4, respectively. Thus our estimated tolerable phase modulation amplitude is $a_2/T_1\leqslant 2.5\times10^{-3}$ in order to eliminate higher order modes and to retain a stable phase space area of about 90% of the bucket area at the 1:1 parametric resonance. The cusp in the bottom plot of Fig. 9 arises from the fact that the synchrotron tune is peaked at a synchrotron amplitude inside the bucket for $T_2/T_1<4$ (see Fig. 2).

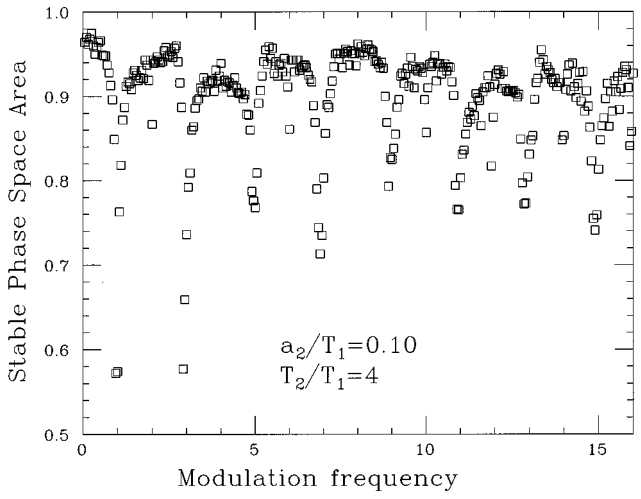

FIG. 7. The stable rf bunch area (in ratio to the bucket area) is plotted as a function of the rf shaking phase modulation frequency (in ratio to the maximum rf frequency). The modulation amplitude is 5% of rf pulse width, i.e., $a_1/T_1=0.10$. The ratio of the rf pulse gap to the pulse width is $T_2/T_1=4$.

C. rf pulse width modulation

The Hamiltonian for the rf pulse width modulation is given by

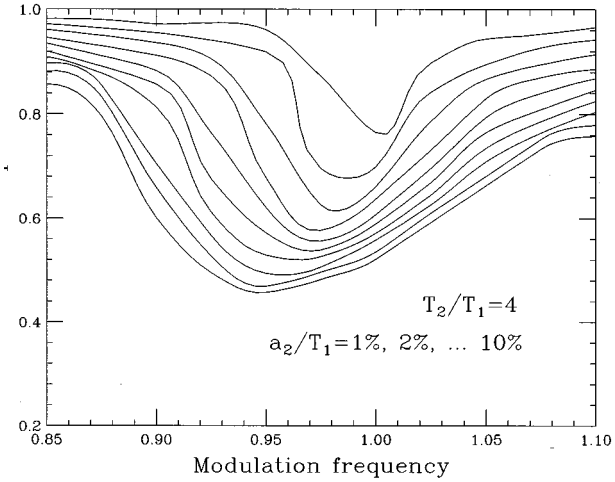

FIG. 8. The stable phase space area (in units of the bucket area) near 1:1 parametric resonance due to the rf phase modulation for $T_2/T_1=4$. The modulation frequency is in units of the maximum rf frequency. The modulation amplitudes are $a_2/T_1=0.01,0.02,\ldots,0.10$, respectively.

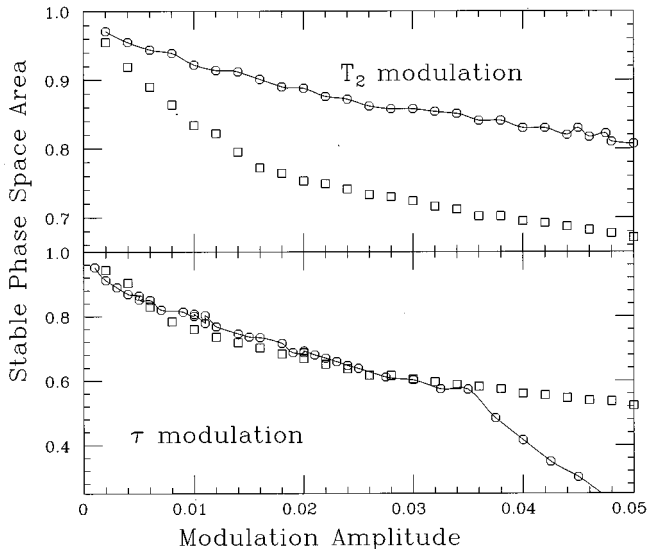

FIG. 9. The stable phase space area (in units of the bucket area) vs the modulation amplitude at 1:1 parametric resonance for the shaking phase modulation (bottom plot) and 2:1 parametric resonance for the breathing phase modulation (top plot). Circular symbols (connected with a line) and rectangular symbols are obtained from the rf parameters with $T_2/T_1=1$ and 4, respectively. The cusp in the rf phase modulation is due to a peaked characteristic of the synchrotron tune.

$$H=H_0+\frac{eV_0a_3}{T_0}f_3(\tau,T_1,T_2)+\Delta H^{(2)}, \tag{3.14}$$

where

$$f_3(\tau,T_1,T_2)=\left[\theta\left(\tau+T_1+\frac{T_2}{2}\right)-\theta\left(\tau-T_1-\frac{T_2}{2}\right)-1\right], \tag{3.15}$$

$$\Delta H^{(2)}=\frac{eV_0a_3}{T_0}\left[\delta\left(\tau+T_1+\frac{T_2}{2}\right)+\delta\left(\tau-T_1-\frac{T_2}{2}\right)\right]+\cdots. \tag{3.16}$$

Since the resonance strength function of f_3 shown in Fig. 3 is zero within the bucket region, parametric resonance will not be excited by the perturbation. Thus the pulse width modulation affects only particles at the bucket boundary without any resonance structure. This can be understood from the total energy variation for particle orbit near the top of the bucket driven by the $\Delta H^{(2)}$ term. It will not affect particles inside the bucket.

IV. rf VOLTAGE MODULATION

When the rf pulse amplitude is modulated, the Hamiltonian for the particle motion becomes

$$H=H_0-\frac{T_1e\Delta V}{T_0}f_0(\tau,T_1,T_2), \tag{4.1}$$

where ΔV is the rf voltage modulation amplitude, and the function f_0 is given by Eq. (2.13). We expand f_0 in action-angle variables, i.e.,

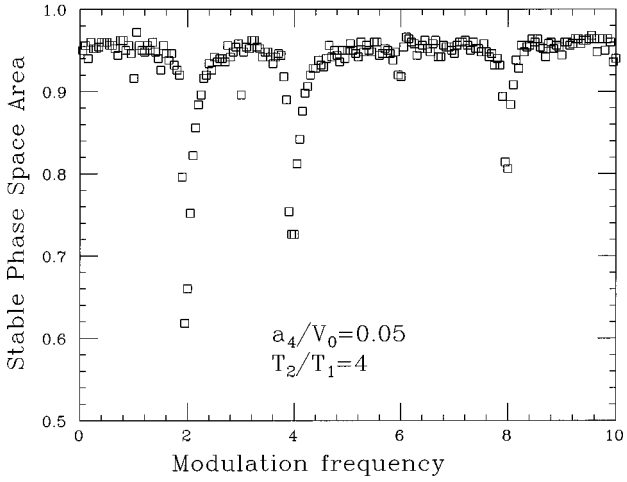

FIG. 10. The stable bucket area (in ratio to the bucket area) vs the rf voltage modulation frequency (in ratio to the maximum synchrotron frequency). The modulation amplitude is 5% of the rf voltage amplitude, i.e., $a_4/V_0=0.05$. The ratio of the rf pulse gap to the pulse width is $T_2/T_1=4$. A small excitation at the 6:1, 10:1, ... is due to the vanishing cosine term in $G_6, G_{10}, \ldots$ for synchrotron orbits at the barrier height.

$$f_0(\tau,T_1,T_2)=\sum_{m=-\infty}^{\infty}G_m(J)e^{im\psi}. \tag{4.2}$$

Since f_0 is an even function of τ, we obtain

$$G_m(J)=\begin{cases}0 & \text{if } m=\text{odd}\\ \dfrac{2(T_2+4W)}{m^2\pi^2T_1}\left[\cos m\psi_c-\dfrac{1}{m\psi_c}\sin m\psi_c\right] & \text{if } m=\text{even.}\end{cases} \tag{4.3}$$

The resonance strength functions satisfy the sum rule theorem

$$\sum_{n=1}^{\infty}|G_{2n}|^2=\frac{16W^3(3T_2+2W)}{45T_1(T_2+4W)^2}. \tag{4.4}$$

The effect of rf voltage modulation is concentrated at low harmonics of the synchrotron sidebands because terms in G_m are proportional to m^{-2} and m^{-3}, respectively.

Figure 10 shows the survival bunch area (in ratio to the bucket area) as a function of $\omega_m/\omega_{s,\max}$ with $\Delta V/V_0=0.05$ and $T_2/T_1=4$. Since the cosine term in $G_6, G_{10}, \ldots$ vanishes for particles with the maximum synchrotron amplitude at the bucket, the effective parametric resonance excitation is much smaller at $\omega_m/\omega_s=6,10, \ldots$ shown in Fig. 10. Although the cosine term in G_2 is also zero, a large resonance strength at the 2:1 resonance arises mainly from the sine term.

Figure 11 shows the stable phase space area (in ratio to the bucket area) vs the modulation frequency (in ratio to the maximum synchrotron frequency) with $T_2=T_1$ and $\Delta V/V_0=0.02,0.04, \ldots,0.20$. Results of many similar simulations show that the tolerable voltage modulation is about $\Delta V/V_0\leqslant 0.01$, in order to attain a minimum of 90% stable phase space area at the 2:1 parametric resonance.

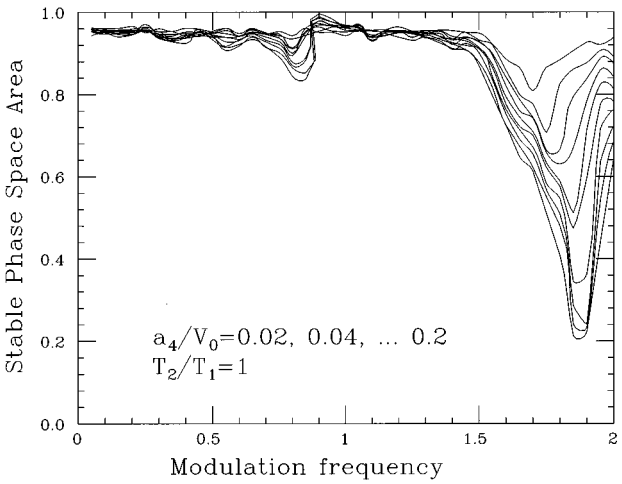

FIG. 11. The stable phase space area (in units of the bucket area) vs the modulation frequency (in units of the maximum synchrotron frequency) for the breathing rf phase modulation with $T_2=T_1$ and $a_1/T_1=0.02,0.04,\ldots,0.20$.

V. TOLERANCE FOR APPLICATIONS

Since the barrier rf system can provide much lower voltage than an ordinary rf cavity system, it is important to evaluate its tolerance in any applications. In the following, we study an example of the Fermilab Recycler which is a fixed energy synchrotron with kinetic energy 8 GeV, circumference 3319.4 m, transition gamma $\gamma_T=20.7$, and a momentum aperture of about 1%. The rms energy spread of entire recycled antiprotons is about 2.7 MeV filled up the whole ring. As the beam is cooled, the resulting 95% momentum spread is about 2 MeV. Allowing a factor of 7 in bunch compression for the newly accumulated antiprotons from the accumulator, the resulting 95% bunch height is 14 MeV. The bucket height for the Recycler is, according to Eq. (2.7),

$$\Delta E_b=13.5(V_0T_1[\text{kV }\mu\text{s}])^{1/2}\ \text{MeV}. \tag{5.1}$$

Thus an integrated field strength of about 2 kV μs is needed to manipulate the recycled antiprotons.

In the conceptual design of this low level rf system, barrier rf waves are generated by digital rf synthesizer [10]. Since the timing jitter in digital frequency synthesizer is small, rf phase modulation due to hardware is negligible. Furthermore, a typical propagation delay time in digital logic circuits is of the order of 10 ns (see for example Ref. [11]). If we assume a typical pulse duration of about $0.5\sim1$ μs and a pessimistic 5% modulational error in the propagation delay time, the actual timing jitter is expected to be about $\Delta t/T_1\leqslant1\times10^{-3}$. Comparing with the constraint for 90% bucket survival derived in Sec. IV, the timing jitter resulting from the barrier rf wave is negligible even when it is at a parametric resonance.

A. Tolerance of phase modulation resulting from synchrobetatron coupling

In the following we analyze the tolerance of orbit length modulation due to the synchrobetatron coupling. In the linear approximation, the orbit length change of the orbiting particle due to an angular kick is equal to $D_x\theta$, where D_x is the dispersion function, and θ is the dipole kick angle. When low frequency modulational angular kicks are applied to the beam, the resulting orbit length change is the integrated orbit variation, i.e., $\Delta C=\oint D_x d\theta$. The resulting timing error in the rf cavity gap is given by

$$\frac{\Delta t}{T_1}=\frac{T_0}{T_1}\frac{\oint D_x d\theta}{2\pi\nu_m C}, \tag{5.2}$$

where C is the circumference of the machine, and $\nu_m=\omega_m/\omega_0$ is the modulation tune. Due to the synchrobetatron coupling, the rf synchronous phase slips in one direction, and accumulates for half of the modulation period before it reverses in the other direction. Because the synchrotron frequency is much smaller than the revolution frequency, the phase error of each term accumulates. The phase modulation amplitude is enhanced by a factor $\omega_0/2\pi\omega_m$. Using the constraint $\Delta t/T_1\leqslant0.0025$ in order to avoid harmful parametric resonances, the tolerable path length error is given by

$$\Delta C=\oint D_x d\theta\approx2\pi\nu_s C\frac{\Delta t}{T_1}\frac{T_1}{T_0}\leqslant3\times10^{-5}\ \text{m} \tag{5.3}$$

for the Recycler, where parameters used are $\nu_s\approx3\times10^{-5}$ (see Fig. 2), $T_1/T_0\approx0.02$, and $C=3319.4$ m. Ground vibration at the frequency of a few Hz is the most important source of the orbit length modulation. Fortunately, ground vibration is mainly vertical, where the corresponding dispersion function is small. However, because of the tight constraint of Eq. (5.3), an active feedback system, e.g., by using a feedback dipole at a high dispersion location, may be needed to eliminate harmful effects of parametric resonances.

B. Constraint on bunch compression

The Recycler storage ring was proposed to recycle the unused antiprotons from the Fermilab Tevatron. At the end of a collider run, unused antiprotons can be decelerated in the Tevatron to 150 GeV. Antiprotons can then be transferred and decelerated in the Main-Injector in about nine pulses and injected into the Recycler for accumulation. After each injection, the recycled antiproton batch must be compressed using the barrier rf wave to make space for the next recycled batch injection as well as the later injection of fresh antiprotons from the Accumulator. The compression rate must be properly determined to eliminate unnecessary particle loss and bunch-area increase. Besides the applications in the antiproton recycling project, the barrier rf wave has been considered for creating a gap in a coasting beam for multipulse injections. The rate at which particles should be pushed by the barrier rf wave is crucial in order not to blow up the longitudinal emittance.

Let $\dot{T}_2<0$ be the compression rate of the barrier rf wave. The change of energy deviation from the synchronous beam energy E_0 after traversing through the barrier rf field region is given by

$$\widehat{\Delta E}_{\text{final}}+\widehat{\Delta E}_{\text{init}}=-2|\dot{T}_2|\frac{\beta^2E_0}{|\eta|}, \tag{5.4}$$

where $\widehat{\Delta E}_{\text{final}}$ and $\widehat{\Delta E}_{\text{init}}$ are the final and initial energy deviations. It is clear from Eq. (5.4) that the energy deviation of a particle with

$$\widehat{\Delta E}=-|\dot{T}_2|\frac{\beta^2E_0}{|\eta|} \tag{5.5}$$

will move at the same speed as the barrier rf wave. This particle will not be affected by the moving barrier. Therefore, in order not to produce empty spaces inside the beam, it is necessary for the barrier rf wave to move with a velocity slower than the drift velocity of particles having the maximum energy spread of the beam $\widehat{\Delta E}_{\text{beam}}$, i.e.,

$$|\dot{T}_{2,\max}|=\frac{|\eta|}{\beta^2E_0}\widehat{\Delta E}_{\text{beam}}. \tag{5.6}$$

It is clear that this result does not depend on the shape of the barrier wave, and it can in fact be used to infer Eq. (5.4).

Even if this condition of Eq. (5.6) is satisfied, empty spaces can still exist if the total compression time for particles with $\widehat{\Delta E}_{\text{beam}}$ does not complete full synchrotron periods. This is because at the time when the compression stops, part of the beam can have an uneven distribution in the phase space. To minimize this effect, the condition that the incremental change of beam energy spread should only be a small fraction of the total beam spread, i.e.,

$$\delta(\widehat{\Delta E}_{\text{beam}})\ll\widehat{\Delta E}_{\text{beam}}, \tag{5.7}$$

where $\delta(\widehat{\Delta E}_{\text{beam}})$ is the increase of energy spread in one complete synchrotron period. Using Eq. (5.4), this requirement becomes

$$|\dot{T}_{2,\max}|\ll\frac{|\eta|}{\beta^2E_0}\hat{\Delta}E_{\text{beam}}, \tag{5.8}$$

which supersedes Eq. (5.6). Again, it is obvious that this constraint is independent of the shape of the barrier wave pulse. If Eq. (5.8) is satisfied, the phase space area should be nearly conserved during the synchrotron phase space manipulations. The phase space area conservation property can be proved as follows.

The amount of compression dT_2 in dN_{syn} synchrotron periods is given by

$$dT_2=\frac{\dot{T}_2}{f_{\text{syn}}}dN_{\text{syn}}, \tag{5.9}$$

where f_{syn} is the synchrotron frequency. Using the synchrotron tune of Eq. (2.11), Eqs. (5.4) and (5.9) can be combined to obtain

$$\frac{dT_2}{T_2}=-\frac{d\widehat{\Delta E}}{\widehat{\Delta E}}\left(1+4\left[\frac{\widehat{\Delta E}}{\Delta E_b}\right]^2\frac{T_1}{T_2}\right). \tag{5.10}$$

When the second term in the round bracket of Eq. (5.10) is small, i.e., a small bunch or a small T_1/T_2 approximation, the equation can be integrated to obtain

$$(T_2\widehat{\Delta E})_{\text{init}}=(T_2\widehat{\Delta E})_{\text{final}}. \tag{5.11}$$

Thus the rectangular part of the phase space is conserved during the compression. The final energy spread of the beam depends only on the amount of compression provided that condition (5.8) is satisfied.

There is another constraint to the compression rate in order to avoid beam loss. If the largest excursion of the beam bunch into the barrier pulse is W, the barrier should not advance by more than T_1-W in each revolution period. From this, we obtain

$$|\dot{T}_2|<\frac{T_1}{T_0}\left[1-\left(\frac{\widehat{\Delta E}_{\text{final}}}{\Delta E_b}\right)^2\right]. \tag{5.12}$$

This condition indicates that the bunch compression does not work for a full bucket.

A preliminary experiment has been carried out at the Brookhaven Alternating Gradient Synchrotron [12], where an empty gap of about $1\,\mu$s was created in 1.3 s using a pair of sinusoidal rf barrier waves. This amounts to $|\dot{T}_2|\sim1.6\times10^{-6}$. Using Eq. (5.8), the constraint of rf compression rate is

$$|\dot{T}_{2,\max}|\leqslant2.7\times10^{-4},$$

where we have used the beam parameters of the AGS with an injection kinetic energy of 1.5 GeV, a transition gamma $\gamma_T=8.5$, and a 0.2% beam momentum spread. Thus the condition given in Eq. (5.8) was well satisfied, and, as expected, no phase space area increase was observed.

A similar bunch beam manipulation for the Recycler at the Fermilab has been contemplated. When antiprotons in the Recycler are cooled to have a small momentum spread, the beam is compressed to accept beam pulses from the antiproton Accumulator. The maximum compression speed is important in preserving the phase space area. Actual experimental tests of beam manipulation schemes are needed in achieving a successful operation of avoiding a hollow beam. Since actual scenarios of beam manipulations are machine dependent, we will not present it here.

VI. CONCLUSION

In conclusion, we analyzed the effect of rf phase and voltage errors on the particle motion in the barrier rf system. We prove analytically that the dynamics of the barrier wave depends only on the total voltage integral in the barrier wave, and is independent of the actual barrier rf wave form. Resonance strength functions and their associated sum rules are derived. We find that the resonance strength function decreases slowly with the mode number. The tolerance of the rf phase and voltage modulation are discussed. We analyze the stability of synchrotron motion for the Fermilab Recycler. The rf phase modulation due to orbit length modulation resulting from ground vibration can be important. Active compensation may be used to compensate for the effect of rf

phase modulation. Some constraints of bunch compression schemes are discussed.

ACKNOWLEDGMENTS

Work was supported in part by U.S. Department of Energy Grants No. DOE-DE-AC02-76CH03000 and No. DOE-92ER40747 and Grant No. NSF PHY-9512832. We thank Chuck Ankenbrandt, David Finley, Jim Griffin, Steve Holmes, Gerry Jackson, Jim MacLachlan, Keith Meisner, and F. Ostiguy for helpful discussions. One of the authors (S.Y.L.) thanks the hospitality of Fermilab colleagues.

APPENDIX: SYNCHROTRON HAMILTONIAN FOR GENERAL BARRIER rf WAVE FORM

From the equations of motion of Eqs. (2.2) and (2.3) , the general synchrotron Hamiltonian for an arbitrary barrier rf wave from is given by

$$H=-\frac{\eta}{2\beta^2E_0}(\Delta E)^2-\frac{\int_0^{\tau}eV(\tau)d\tau}{T_0}. \tag{A1}$$

Thus the maximum off-energy bucket height can be easily derived to be

$$\Delta E_b=\left(\frac{2\beta^2E_0}{|\eta|}\frac{\left|\int_{T_2/2}^{T_2/2+T_1}eV(\tau)d\tau\right|}{T_0}\right)^{1/2}, \tag{A2}$$

where T_1 is the width of the barrier rf wave form. Since the barrier rf Hamiltonian is time independent, an invariant torus has a constant Hamiltonian value. The W parameter for a torus is defined by

$$\frac{|\eta|}{2\beta^2E_0}(\widehat{\Delta E})^2=\frac{\left|\int_{T_2/2}^{T_2/2+W}eV(\tau)d\tau\right|}{T_0}. \tag{A3}$$

The synchrotron period of a Hamiltonian torus can be written as

$$T_s=2\frac{T_2}{|\eta|}\left(\frac{\beta^2E_0}{|\widehat{\Delta E}|}\right)+4T_c, \tag{A4}$$

where T_c is given by

$$T_c=\frac{\beta^2E_0}{|\eta|}\int_0^W\frac{d\tau}{\sqrt{(\widehat{\Delta E})^2-\frac{2\beta^2E_0}{|\eta|T_0}\int_{T_2/2}^{T_2/2+\tau}eV(\tau')d\tau'}}. \tag{A5}$$

Clearly, all physical quantities depend essentially on $\int V(\tau)d\tau$. Thus the essential physics is independent of the exact shape of the barrier rf wave.

[1] G. Jackson (private communications). Assuming 7 h of store duration, about 1.5×10^{12} antiprotons will be recycled with a total 95% phase space area about 108 eV s: see Fermilab Recycler Ring Design Report, April, 1996.

[2] J. Griffin, C. Ankenbrandt, J. A. MacLachlan, and A. Moretti, IEEE Trans. Nucl Sci. **NS30**, 3502 (1983); V. K. Bharadwaj, J. E. Griffin, D. J. Harding, and J. A. MacLachlan, *ibid.* **NS34**, 1025 (1987).

[3] M. Ellison *et al.*, Phys. Rev. Lett. **70**, 591 (1993); H. Huang *et al.*, Phys. Rev. E **48**, 4678 (1993).

[4] Y. Wang *et al.*, Phys. Rev. E **49**, 1610 (1994); M. Syphers *et al.*, Phys. Rev. Lett. **71**, 719 (1993).

[5] S. Y. Lee, Phys. Rev. E **49**, 5706 (1994)

[6] D. Li *et al.*, Phys. Rev. E **48**, R1638 (1993); Nucl. Instrum. Methods Phys. Res. Sect. A **364**, 205 (1995).

[7] S. Y. Lee *et al.*, Phys. Rev. E **49**, 5717 (1994); J. Y. Liu *et al.*, *ibid.* **50**, R3349 (1994); Part. Accel. **49**, 221 (1995).

[8] S. Y. Lee, in *Accelerator Physics at the SSC*, edited by Y. Yan and M. Syphers, AIP Conf. Proc. No. 326 (AIP, New York, 1995), p. 13.

[9] The Poincaré surface of section is obtained by plotting a phase space point every $1/\nu_m$ orbital revolutions.

[10] K. Meisner (private communication).

[11] R. S. Sandige, *Digital Concepts Using Standard Integrated Circuits* (McGraw-Hill, New York, 1978).

[12] T. Roser (private communication).